



HAL
open science

Rebit channel classification and its applications to colour perception

Michele Aldé, Michel Berthier, Edoardo Provenzi

► **To cite this version:**

Michele Aldé, Michel Berthier, Edoardo Provenzi. Rebit channel classification and its applications to colour perception. 2023. hal-04039881v1

HAL Id: hal-04039881

<https://hal.science/hal-04039881v1>

Preprint submitted on 21 Mar 2023 (v1), last revised 11 Nov 2023 (v2)

HAL is a multi-disciplinary open access archive for the deposit and dissemination of scientific research documents, whether they are published or not. The documents may come from teaching and research institutions in France or abroad, or from public or private research centers.

L'archive ouverte pluridisciplinaire **HAL**, est destinée au dépôt et à la diffusion de documents scientifiques de niveau recherche, publiés ou non, émanant des établissements d'enseignement et de recherche français ou étrangers, des laboratoires publics ou privés.

Rebit channel classification and its applications to colour perception

Michele Aldé^{*1}, Michel Berthier^{†2} and Edoardo Provenzi^{‡3}

¹Università degli studi di Milano, Dipartimento di matematica, via Saldini 50, 20133 Milano, Italy.

²Laboratoire MIA, Batiment Pascal, Pôle Sciences et Technologie, Université de La Rochelle, 23, Avenue A. Einstein, BP 33060, 17031 La Rochelle cedex, France.

³Université de Bordeaux, CNRS, Bordeaux INP, IMB, UMR 5251, F-33400, 351 Cours de la Libération, Talence, France

Abstract

The classification of qubit channels is known since 2002. However, that of rebit channels has never been studied so far, probably due to the scarcity of concrete rebit examples. In this paper we fill the two gaps by exhibiting both the complete rebit channel classification and also by discussing its relevancy in a recent colour perception theory based on quantum information. In particular, we show that rebit channels can be used to determine the individual chromatic state space of human observers, including those with colour deficiencies. Moreover, we propose a qualitative explanation for the perceptual phenomenon of visual adaptation to a non-neutral illuminant.

Keywords: Quantum information, effects, rebit channels, colour perception, individual colour space

1 Introduction

Quantum channels represent the most general transformations between states of interacting, or open, quantum systems. Their classification is a complicated research topic and can only be achieved in very special cases. An example of paramount importance is represented by qubit systems, whose channel classification has been exhibited in [16].

Up to the authors' knowledge, the analogous result for rebit systems has never been obtained. In the first part of this paper we provide the complete classification of rebit quantum channels showing that the technique developed in [16], based on Choi's theorem, cannot be used for the rebit case, but an alternative strategy based on the χ -map representation must be considered.

While qubits are ubiquitous in quantum information, rebits remained for many decades a very interesting but abstract research topic, see for instance [20]. This is likely to be the cause underlying the lack of interest in the rebit channel classification. For this reason, we deem important to show the relevance of our mathematical results in the concrete framework offered by a recent quantum-like colour perception theory proposed in the papers [4, 2, 7, 5, 3, 8, 6], where the space of the so-called perceptual chromatic states coincides with the state space of a rebit system.

By interpreting colour perception as the result of the interaction between a human observer and either a light stimulus or a patch lit by an illuminant, we show that the classification of rebit

*michele.alde@studenti.unimi.it

†michel.berthier@univ-lr.fr

‡edoardo.provenzi@math.u-bordeaux.fr

channels permits to characterise individual colour perception and to incorporate in the model also observers with colour deficiencies. Moreover, we discuss how rebit channels can help us understanding the phenomenon of adaptation to non-neutral illuminants not too different from daylight and why, instead, humans fail to adapt to narrowband illuminant conditions.

The plan of the paper is the following: we start in section 2 by briefly recalling the basic terminology and mathematical results about open quantum systems, then we pass to the rebit channel classification in section 3, which will be subdivided in several subsection for the sake of a smoother reading. The second part of the paper, devoted to applications, will start in section 4, where we will recall the most important results of the quantum-like colour perception model. The usefulness of the rebit quantum channel classification will be discussed in section 5. Finally, in section 6 we will conclude the paper with some perspectives for future investigations.

2 Terminology and mathematical results about open quantum systems

Here we introduce the terminology and the known mathematical results of the theory of composite quantum systems that will be used in the rest of the paper. Unless otherwise stated, the main reference for all the results that will be quoted is [11]. All the Hilbert spaces that we will deal with are implicitly assumed to be *finite-dimensional* and *real*.

Given a quantum system S , if A and B are two identifiable parts of it, i.e. two subsystems on which we are able to perform experiments to address the properties of A and B individually, then we say that the S is the composite system of A and B and we write $S = A + B$. If \mathcal{H}_A and \mathcal{H}_B are the Hilbert state spaces underlying the systems A and B , respectively, then the quantum state space of $A + B$ is $\mathcal{H}_A \otimes \mathcal{H}_B$.

If A is not isolated, i.e. it can interact with B , then we say that A is an open quantum system and B is its environment. If $L(\mathcal{H}_A)$ denotes the vector space of linear operators on \mathcal{H}_A , then a linear map $C : L(\mathcal{H}_A) \rightarrow L(\mathcal{H}_A)$ is said to be a *channel* if it is trace preserving and completely positive. This last request corresponds to demand not only that ϕ is positive, i.e. it respects the positivity¹ of operators on \mathcal{H}_A but also that its extension, i.e. the map $C \otimes id_B : L(\mathcal{H}_A \otimes \mathcal{H}_B) \rightarrow L(\mathcal{H}_A \otimes \mathcal{H}_B)$, is positive. The requests defining a channel C are the minimal ones to guarantee that C maps states in states and that C does not introduce non-meaningful negative probabilities when experiments on the composite quantum system $A + B$ are performed. To simplify the notation, let us denote from now on \mathcal{H}_A as \mathcal{H} .

An important class of channels is represented by the orthogonal ones: given an orthogonal operator $O \in L(\mathcal{H})$, the *orthogonal channel* associated to O is the map $\sigma_O : L(\mathcal{H}) \rightarrow L(\mathcal{H})$ such that, for all $T \in L(\mathcal{H})$, $\sigma_O(T) := OT O^t$. Orthogonal channels are *unital*, i.e. they map the identity into itself, moreover, they form a group w.r.t. functional composition.

For the classification of channels their matrix representations turn out to be extremely useful. The most basic of these representations can be obtained by equipping $L(\mathcal{H})$ with the Hilbert-Schmidt (HS) product, i.e. $\langle T, S \rangle_{\text{HS}} = \text{Tr}(S^t T)$ for all $T, S \in L(\mathcal{H})$, and fixing an orthonormal basis $(E_j)_{j=0}^{d^2-1}$ of operators of $L(\mathcal{H})$. This permits to decompose $T \in L(\mathcal{H})$ as follows

$$T = \sum_{j=0}^{d^2-1} t_j^T E_j = \sum_{j=0}^{d^2-1} \text{Tr}(E_j^t T) E_j \quad (1)$$

and to uniquely associate it to the vector $\mathbf{t}^T = (t_j^T)_{j=0}^{d^2-1} \in \mathbb{R}^{d^2}$. If $C : L(\mathcal{H}) \rightarrow L(\mathcal{H})$ is a channel, then, by linearity, it follows that

$$C(T) = \sum_{j=0}^{d^2-1} t_j^{C(T)} E_j, \quad (2)$$

¹ $T \in L(\mathcal{H}_A)$ is positive if, for all $x \in \mathcal{H}_A$, $\langle x, Tx \rangle \geq 0$, where $\langle \cdot, \cdot \rangle$ is the inner product of \mathcal{H}_A .

where

$$\mathbf{t}_j^{C(T)} = \sum_{k=0}^{d^2-1} C_{jk} t_k^T \quad \text{and} \quad C_{jk} = \text{Tr}(E_j^t C(E_k)). \quad (3)$$

$\mathbf{t}^{C(T)} = (t_j^{C(T)})_{j=0}^{d^2-1}$ is the vector in \mathbb{R}^{d^2} uniquely associated to $C(T)$ w.r.t. the basis $(E_j)_{j=0}^{d^2-1}$.

A more sophisticated representation than the one just introduced is the so-called χ -*matrix representation*, which will turn out to be a key ingredient for the rebit channel classification. This representation is introduced by considering the $(d^2 \times d^2)$ -dimensional vector space $L(L(\mathcal{H}))$ of linear maps on $L(\mathcal{H})$ endowed with the following inner product inherited by the Hilbert-Schmidt product on $L(\mathcal{H})$:

$$\langle \Psi, \Phi \rangle := \sum_{j=0}^{d^2-1} \langle \Psi(E_j), \Phi(E_j) \rangle_{\text{HS}}, \quad \forall \Psi, \Phi \in L(L(\mathcal{H})). \quad (4)$$

In the rebit channel classification, we will be interested in the action of channels on density matrices, which are symmetric, hence it is more useful to replace $L(L(\mathcal{H}))$ with $L(\text{Sym}(\mathcal{H}))$, where $\text{Sym}(\mathcal{H}) \subset L(\mathcal{H})$ is the vector subspace of dimension $N = d(d+1)/2$ of symmetric linear operators on \mathcal{H} .

Given an orthonormal basis $(E_j)_{j=0}^{N-1}$ of operators of $\text{Sym}(\mathcal{H})$, an orthonormal basis $(F_{rs})_{r,s=0}^{N-1}$ for $L(\text{Sym}(\mathcal{H}))$ is defined by

$$F_{rs}(T) := E_r T E_s^t, \quad \forall T \in \text{Sym}(\mathcal{H}), \quad (5)$$

so we can decompose a channel C on $(F_{rs})_{r,s=0}^{N-1}$ as

$$C = \sum_{r,s=0}^{N-1} \chi_{rs} F_{rs}, \quad (6)$$

where the coefficients χ_{rs} are obtained via inner product of C with the basis elements F_{rs} and can be written explicitly as follows

$$\chi_{rs} = \sum_{j,k=0}^{N-1} C_{jk} \text{Tr}(E_j E_s E_k^t E_r^t), \quad (7)$$

with C_{jk} as in eq. (3). The χ -matrix uniquely associated to C is $\chi_C := (\chi_{rs})_{r,s=0}^{N-1}$ and it has the property that C is completely positive if and only if χ_C is positive semi-definite, see [11] page 206.

The last matrix representation that we need to recall is the *Bloch representation*, which relies on the choice of a *Bloch basis* $E_0 := I_d \cup \vec{E}$, $\vec{E} := (E_1, \dots, E_{N-1})$, i.e. an orthogonal basis (w.r.t. the Hilbert-Schmidt product) of symmetric traceless operators on \mathcal{H} such that $\|E_k\|_{\text{HS}}^2 = \|E_0\|_{\text{HS}}^2 = d$ for all $k = 1, \dots, N-1$, which induces the so-called *Bloch decomposition*:

$$T = \frac{1}{d}(\text{Tr}(T)I_d + \mathbf{v}^T \cdot \vec{E}) = \frac{1}{d}(\text{Tr}(T)I_d + \sum_{k=1}^{N-1} v_k^T E_k), \quad (8)$$

where $\mathbf{v}^T \in \mathbb{R}^{N-1}$ is called *Bloch vector* and has components $v_k^T = \text{Tr}(E_k T)$, $k = 1, \dots, N-1$.

The relationship between the vector \mathbf{t}^T and the Bloch vector \mathbf{v}^T is the following

$$\mathbf{t}^T = \frac{1}{d}(\text{Tr}(T), \mathbf{v}^T). \quad (9)$$

Given a channel C , the relationship between the vector $\mathbf{t}^{C(T)}$ and the Bloch vector $\mathbf{v}^{C(T)}$ becomes (see [11] page 205)

$$\mathbf{t}^T = \frac{1}{d}(\text{Tr}(T), \mathbf{v}^{C(T)}), \quad \text{with} \quad \mathbf{v}^{C(T)} = \mathbf{w} + A\mathbf{v}^T, \quad (10)$$

where the components of the vector $\mathbf{w} \in \mathbb{R}^{N-1}$ and the entries of the matrix $A \in M(N-1, \mathbb{R})$ are

$$w_j = \text{Tr}(T)C_{j0}, \quad A_{jk} = C_{jk}, \quad j, k = 1, \dots, N-1. \quad (11)$$

Two features of the Bloch representation can be singled out: after the action of a channel, *the first component of \mathbf{t}^T remains invariant*, while *the Bloch vector undergoes an affine transformation*.

For later purposes, we remark a third property: *whenever a linear map leaves the first component of \mathbf{t}^T invariant, for all T , that map is trace-preserving*.

For orthogonal channel we can say more, as stated in the following theorem, see [11] page 205.

Theorem 2.1 *If C is a unitary channel σ_O , then*

$$\mathbf{v}^{\sigma_O(T)} = R_O \mathbf{v}^T, \quad R_O \in \text{SO}(N-1), \quad (12)$$

with:

$$(R_O)_{jk} = \frac{1}{d} \text{Tr}(E_j O E_k O^t), \quad j, k = 1, \dots, N-1, \quad (13)$$

i.e. *the Bloch vector of $T \in L(\mathcal{H})$ undergoes a rotation after the application of an orthogonal channel*:

$$\sigma_O(T) = \frac{1}{d} (I_d + R_O \mathbf{v}^T \cdot \vec{E}). \quad (14)$$

3 Classification of rebit channels

In this section we will carry out the complete classification of rebit channels. Due to the length of this procedure, we have subdivided the section in several subsections to facilitate the reading.

3.1 The first step: decomposition of a rebit channel in the orthogonal and diagonal parts

To study the classification of rebit channels we fix $\mathcal{H} = \mathbb{R}^2$ and the Bloch basis $(\sigma_j)_{j=0}^2$, where σ_0 is I_2 and σ_1, σ_2 are the (symmetric and traceless) real Pauli matrices:

$$\sigma_1 = \begin{pmatrix} 1 & 0 \\ 0 & -1 \end{pmatrix}, \quad \sigma_2 = \begin{pmatrix} 0 & 1 \\ 1 & 0 \end{pmatrix}. \quad (15)$$

Moreover, instead of considering a general operator T , we will deal directly with density matrices, i.e. positive unit-trace operators $\rho \in L(\mathbb{R}^2)$ representing rebit states. As it is well-known, the convex set of density matrices $\mathcal{S}(\mathbb{R}^2)$ of the rebit is parametrized by the points of the unit disk $\mathcal{D} \subset \mathbb{R}^2$, also referred to as the *Bloch disk*.

Since $d = \dim_{\mathbb{R}}(\mathcal{H}) = 2$, all the orthogonal channels are exhausted by rotation matrices². Moreover, since $d = 2$, we have that $N = 2(2+1)/2 = 3$ and so the rotation matrix R appearing in theorem 2.1 belongs to $\text{SO}(2)$ and labels orthogonal channels $\sigma_{\Omega_R} : \mathcal{S}(\mathbb{R}^2) \rightarrow \mathcal{S}(\mathbb{R}^2)$ such that

$$\sigma_{\Omega_R}(\rho) := \Omega_R \rho \Omega_R^t, \quad (16)$$

with $\Omega_R^t = \Omega_R^{-1}$ and, thanks to eq. (13), $R_{jk} = \text{Tr}(\sigma_j \Omega_R \sigma_k \Omega_R^t)/2$, for all $j, k = 1, 2$.

Finally, a generic channel C induces an affine transformation of the Bloch vector $\mathbf{v}^\rho \in \mathcal{D}$, so there exist $\mathbf{w} \in \mathbb{R}^2$ and $A \in M(2, \mathbb{R})$ such that

$$C(\rho) = \frac{1}{2} (I_2 + (\mathbf{w} + A \mathbf{v}^\rho) \cdot \vec{\sigma}), \quad (17)$$

or, if C is unital,

$$C(\rho) = \frac{1}{2} (I_2 + A \mathbf{v}^\rho \cdot \vec{\sigma}). \quad (18)$$

²As proven in [11], this holds only in dimension 2, so either for the rebit or the qubit, for which $\mathcal{H} = \mathbb{C}^2$ and $\dim_{\mathbb{C}}(\mathcal{H}) = 2$.

The information recalled above imply that we can classify the rebit channels by determining what are the possible matrices A and vectors \mathbf{w} that may appear in eq. (17) such that C remains a channel. Of course, the classification would be greatly simplified if the matrix A were diagonal or at least diagonalizable, however this may not be achievable. Instead, it is always possible to write a singular value decomposition of A :

$$A = O_1 \Sigma O_2^t, \quad (19)$$

where $O_1, O_2 \in \text{O}(2)$ and $\Sigma = \text{diag}(\mu_1, \mu_2)$, where $\mu_1, \mu_2 \in [0, +\infty)$ are the singular values of A .

Adapting the strategy used in [16] to the rebit case, we now show how it is possible to handle eq. (19) in order to understand how rebit channels act on the unit disk, up to a rotation, by replacing A with a diagonal matrix D , originated from Σ , which is able to encompass also the general case in which the diagonal entries do not have the same sign.

We start by the basic remark that $O_j \in \text{O}(2)$ can be seen as the product of a rotation matrix $R_j \in \text{SO}(2)$ with the matrix

$$\mathcal{I} = \begin{cases} \text{diag}(1, 1) \equiv I_2 & \text{if } O_j \in \text{SO}(2) \\ \text{diag}(1, -1) \equiv I_2' & \text{if } O_j \in \text{O}(2) \setminus \text{SO}(2) \end{cases}, \quad (20)$$

the second case representing a reflection around the horizontal axis.

If both O_1 and O_2 belong to $\text{SO}(2)$ or to $\text{O}(2) \setminus \text{SO}(2)$ then we can rewrite $O_j = R_j \mathcal{I}$ in eq. (19) where \mathcal{I} is either the identity or the reflection, respectively. Taking into account that $\mathcal{I}^2 = I_2$ in both cases and that Σ and \mathcal{I} commute, we obtain

$$A = R_1 \mathcal{I} \Sigma \mathcal{I} R_2^t = R_1 \Sigma R_2^t. \quad (21)$$

If, instead, $O_i \in \text{SO}(2)$ and $O_j \in \text{O}(2) \setminus \text{SO}(2)$, with $i, j \in \{1, 2\}$, $i \neq j$, then eq. (19) becomes

$$A = R_1 \Sigma' R_2^t, \quad (22)$$

where $\Sigma' := I_2' \Sigma = \Sigma I_2' = \text{diag}(\mu_1, -\mu_2)$, which is *no longer positive semi-definite*.

By introducing the decomposition of the identity $R_2 R_2^t$ after R_1 in the two previous expressions of A , we get either $A = R_1 R_2^t R_2 \Sigma R_2^t$ or $A = R_1 R_2^t R_2 \Sigma' R_2^t$, but

$$R := R_1 R_2^t \quad (23)$$

belongs to $\text{SO}(2)$ and

$$S := \begin{cases} R_2 \Sigma R_2^t \\ \text{or} \\ R_2 \Sigma' R_2^t \end{cases} \quad (24)$$

is such that $S^t = S$, i.e. it is a real symmetric matrix and, as such, diagonalizable.

Notice that S is not necessarily a positive semi-definite matrix since the conjugation of Σ or Σ' with the rotation matrix R_2 does not affect their eigenvalues and Σ' is not positive-definite. Hence, if $\mathcal{O} \in \text{O}(2)$ is the orthogonal matrix that diagonalizes S , then

$$A = R \mathcal{O} D \mathcal{O}^t, \quad (25)$$

where $D = \text{diag}(\lambda_1, \lambda_2)$, with $\lambda_j \in \mathbb{R}$ and $|\lambda_j| = \mu_j$, $j = 1, 2$. Now we can repeat the same argument used above, i.e. we can write $\mathcal{O} = R_3 \mathcal{I}$, with $R_3 \in \text{SO}(2)$, so that eq. (25) becomes $A = R R_3 \mathcal{I} D \mathcal{I} R_3^t = R R_3 D R_3^t$.

By defining $\mathcal{R}_1 := R R_3 \in \text{SO}(2)$ and $\mathcal{R}_2 := R_3^t \in \text{SO}(2)$ we can finally write:

$$A = \mathcal{R}_1 D \mathcal{R}_2. \quad (26)$$

A natural question that arises now is that if the matrix factorization $A = \mathcal{R}_1 D \mathcal{R}_2$ implies an analogous channel factorization, the answer is positive thanks to the fact that \mathcal{R}_1 and \mathcal{R}_2 are special

orthogonal matrices and we are working in dimension 2, so they are automatically associated to orthogonal channels $\sigma_{\Omega_{\mathcal{R}_1}}$ and $\sigma_{\Omega_{\mathcal{R}_2}}$, which simply act on a Bloch vector via the matrix \mathcal{R}_1 and \mathcal{R}_2 , respectively. So, the only degree of freedom that we have is in the definition of the channel corresponding to the matrix D . It is quite simple to recognize that the sequential transformation that must be applied to the Bloch vector \mathbf{v}^ρ in order to obtain formula (17) with $A = \mathcal{R}_1 D \mathcal{R}_2$ is the following:

$$\mathbf{v}^\rho \xrightarrow{\sigma_{\Omega_{\mathcal{R}_2}}} \mathcal{R}_2 \mathbf{v}^\rho \xrightarrow{C_D} \mathcal{R}_1^t \mathbf{w} + D \mathcal{R}_2 \mathbf{v}^\rho \xrightarrow{\sigma_{\Omega_{\mathcal{R}_1}}} \mathcal{R}_1 (\mathcal{R}_1^t \mathbf{w} + D \mathcal{R}_2 \mathbf{v}^\rho) = \mathbf{w} + \mathcal{R}_1 D \mathcal{R}_2 \mathbf{v}^\rho. \quad (27)$$

The action of the second transformation on the density matrix ρ is

$$C_D(\rho) = C_D \left(\frac{1}{2} (I_2 + \mathbf{v}^\rho \cdot \vec{\sigma}) \right) := \begin{cases} \frac{1}{2} (I_2 + (\mathcal{R}_1^t \mathbf{w} + D \mathcal{R}_2 \mathbf{v}^\rho) \cdot \vec{\sigma}) & \text{if } C \text{ is not unital} \\ \frac{1}{2} (I_2 + D \mathcal{R}_2 \mathbf{v}^\rho \cdot \vec{\sigma}) & \text{if } C \text{ is unital.} \end{cases} \quad (28)$$

We can summarize what we have found in the following theorem.

Theorem 3.1 *For every rebit channel C there exist two rotation matrices $\mathcal{R}_1, \mathcal{R}_2 \in \text{SO}(2)$ and a diagonal matrix $D = \text{diag}(\lambda_1, \lambda_2)$, with $\lambda_1, \lambda_2 \in \mathbb{R}$, such that C can be written as:*

$$C = \sigma_{\Omega_{\mathcal{R}_1}} \circ C_D \circ \sigma_{\Omega_{\mathcal{R}_2}}, \quad (29)$$

where $\sigma_{\Omega_{\mathcal{R}_j}}$ are the orthogonal channels associated to \mathcal{R}_j , $j = 1, 2$, and C_D is defined as in eq. (28).

As a consequence of this theorem, the rebit channels classification is equivalent to the determination of the constraints that must be satisfied by the map C_D in order to be a channel. These constraints will clearly affect the shift vector \mathbf{w} and the entries of the diagonal matrix D .

The discussion of these constraints is long and quite technical and we postpone it to subsection 3.3. Instead, in the next subsection we carry out the much simpler analysis of the possible geometric deformations of the unit disk \mathcal{D} , the state space of the rebit, induced by channels.

3.2 Geometric deformation of the state space by rebit channels

The action of the orthogonal channels corresponds simply to a rotation of the Bloch vector \mathbf{v}^ρ and the shift vector \mathbf{w} . So, geometrically speaking, the only non-trivial part of the decomposition written in eq. (29) is represented by action of C_D .

To avoid an unnecessary complicated notation and keep the analysis as simple as possible, we will rewrite $\mathcal{R}_2 \mathbf{v}^\rho$ and $\mathcal{R}_1^t \mathbf{w}$ simply as $\mathbf{v}^\rho = (v_1^\rho, v_2^\rho)$ and $\mathbf{w} = (w_1, w_2)$, respectively. Using this simplified notation, we can write the modification of the vector $\mathbf{t}^\rho = \frac{1}{2}(1, v_1^\rho, v_2^\rho)$ by C_D as follows:

$$\mathbf{t}^{C_D(\rho)} = \frac{1}{2} \left(1, v_1^{C_D(\rho)}, v_2^{C_D(\rho)} \right) = \frac{1}{2} (1, w_1 + \lambda_1 v_1^\rho, w_2 + \lambda_2 v_2^\rho), \quad (30)$$

or

$$\mathbf{t}^{C_D(\rho)} = \frac{1}{2} \left(1, v_1^{C_D(\rho)}, v_2^{C_D(\rho)} \right) = \frac{1}{2} (1, \lambda_1 v_1^\rho, \lambda_2 v_2^\rho), \quad (31)$$

in the case of unital channels.

Let us analyze the latter case first: the action of C_D on \mathbf{t}^ρ is represented in matrix form by

$$\begin{pmatrix} 1 & 0 & 0 \\ 0 & \lambda_1 & 0 \\ 0 & 0 & \lambda_2 \end{pmatrix} = \begin{pmatrix} 1 & \mathbf{0} \\ \mathbf{0} & D \end{pmatrix}, \quad (32)$$

moreover, on one side we have that $\left(v_1^{C_D(\rho)}\right)^2 + \left(v_2^{C_D(\rho)}\right)^2 \leq 1$ to assure the positivity of C_D , i.e. that $\mathbf{v}^{C_D(\rho)}$ is still a state, and, on the other side, from (31) we have that $v_j = v_j^{C_D(\rho)}/\lambda_j$, $j = 1, 2$, so the constraint $(v_1^\rho)^2 + (v_2^\rho)^2 \leq 1$ is translated into the inequality

$$\left(\frac{v_1^{C_D(\rho)}}{\lambda_1}\right)^2 + \left(\frac{v_2^{C_D(\rho)}}{\lambda_2}\right)^2 \leq 1. \quad (33)$$

This means that C_D maps the set of rebit states \mathcal{D} in the two dimensional closed ellipsoid embedded in \mathcal{D} represented by equation (33). On its border we find the images by C_D of the pure states of the rebit, parametrized by the elements of the unit circle. Since λ_1 and λ_2 are the semi-axes of this ellipsoid, they must verify

$$|\lambda_j| \leq 1, \quad j = 1, 2. \quad (34)$$

The centre of the Bloch disk remains fixed by the action of C_D only if C is unital. In the more general case of a non-unital channel C we have, by eq. (30), that the action of C_D on \mathbf{t}^ρ can be represented via the affine matrix

$$\mathbb{A} = \begin{pmatrix} 1 & 0 & 0 \\ w_1 & \lambda_1 & 0 \\ w_2 & 0 & \lambda_2 \end{pmatrix} = \begin{pmatrix} 1 & \mathbf{0} \\ \mathbf{w} & D \end{pmatrix} \quad (35)$$

and the image of the Bloch disk under the action of C_D is an ellipsoid with origin of the semi-axes given by (w_1, w_2) and with analytic expression given by:

$$\left(\frac{v_1^{C_D(\rho)} - w_1}{\lambda_1}\right)^2 + \left(\frac{v_2^{C_D(\rho)} - w_2}{\lambda_2}\right)^2 \leq 1, \quad (36)$$

Again, to guarantee the positivity of C_D , i.e. that the constraints defining states are still valid, we must have

$$|w_j| \leq 1, \quad j = 1, 2. \quad (37)$$

λ_1 and λ_2 will be called *scale coefficients*, while we will refer to w_1 and w_2 as *shift coefficients*.

3.3 Analytical constraints on C_D to be a channel

In order to be a channel, C_D must be completely positive and trace-preserving. This last property is easily seen to be satisfied, in fact the first row of the matrix appearing in formula (35) is $(1, 0, 0)$, hence it leaves the first component of the vector \mathbf{t}^ρ unaltered. In section 2 we have seen that this implies that C_D is trace-preserving. So, only complete positivity must be examined.

In [16], necessary and sufficient conditions for the complete positivity in the qubit case have been established by using Choi's theorem. For that, it is essential to rewrite the four matrices E_{jk} , $j, k = 1, 2$, of the canonical basis of $M(2, \mathbb{C})$ as a linear combination of the identity plus the *three* Pauli matrices, including the one with complex entries. However, in the rebit case we have at disposal only the identity plus the *two* real Pauli matrices and so this technique cannot be pursued any longer. Hence, other strategies must be considered.

In what follows we will show that the χ -matrix representation recalled in section 2 can be used instead of the Choi theorem to establish necessary and sufficient conditions for the complete positivity of the map C_D .

In order to build the χ -matrix associated to C_D it is convenient to fix the orthonormal Bloch basis of $\mathcal{H}(2, \mathbb{R})$, i.e. $(\sigma_0, \sigma_1, \sigma_2)/\sqrt{2}$. Thanks to eqs. (7) and (35) we get

$$\begin{aligned} \chi_{r,s} &= \frac{1}{4} \sum_{k=0}^2 \text{Tr}[\sigma_s \sigma_k \sigma_r C_D(\sigma_k)] \\ &= \frac{1}{4} \left[\text{Tr}(\sigma_s \sigma_r (I_2 + w_1 \sigma_1 + w_2 \sigma_2)) + \lambda_1 \text{Tr}(\sigma_s \sigma_1 \sigma_r \sigma_1) + \lambda_2 \text{Tr}(\sigma_s \sigma_2 \sigma_r \sigma_2) \right]. \end{aligned} \quad (38)$$

The straightforward computation of the matrix elements gives

$$\chi_{C_D}(\lambda_1, \lambda_2, w_1, w_2) = \frac{1}{2} \begin{pmatrix} 1 + \lambda_1 + \lambda_2 & w_1 & w_2 \\ w_1 & 1 + \lambda_1 - \lambda_2 & 0 \\ w_2 & 0 & 1 - \lambda_1 + \lambda_2 \end{pmatrix}. \quad (39)$$

As recalled in section 2, the complete positivity of C_D is equivalent to the positive semi-definiteness of χ_{C_D} . Being a real symmetric matrix, its eigenvalues are all real and so χ_{C_D} is positive semi-definite if and only if all its eigenvalues are non-negative. We will conduct the analysis of positive semi-definiteness following an increasing order of complexity.

3.3.1 The unital case ($w_1 = w_2 = 0$)

Unital rebit channels leave the centre of the Bloch disk invariant, so they have a null shift vector $\mathbf{w} = (w_1, w_2) = \mathbf{0}$.

This means that the χ -matrix in this case reduces to the following diagonal form

$$\chi_{C_D}(\lambda_1, \lambda_2) = \frac{1}{2} \begin{pmatrix} 1 + \lambda_1 + \lambda_2 & 0 & 0 \\ 0 & 1 + \lambda_1 - \lambda_2 & 0 \\ 0 & 0 & 1 - \lambda_1 + \lambda_2 \end{pmatrix}.$$

Its eigenvalues are therefore its three diagonal elements, i.e.

$$q_0 := \frac{1}{2}(1 + \lambda_1 + \lambda_2), \quad q_1 := \frac{1}{2}(1 + \lambda_1 - \lambda_2), \quad q_2 := \frac{1}{2}(1 - \lambda_1 + \lambda_2) \quad (40)$$

and so, C_D is completely positive if and only if

$$\begin{cases} \lambda_2 \geq -1 \pm \lambda_1 \\ \lambda_2 \leq 1 + \lambda_1 \end{cases}. \quad (41)$$

Since $(\lambda_1, \lambda_2) \in [-1, 1] \times [-1, 1] \subset \mathbb{R}^2$, the three inequalities appearing in the system (41) define the admissibility region \mathcal{P} for the parameters, which lies inside the pentagon of Figure 1.

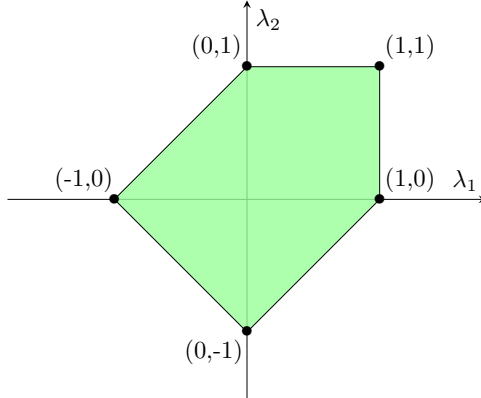


Figure 1: Admissibility region \mathcal{P} for the parameters λ_1 and λ_2 to guarantee the complete positivity of the map C_D in the unital case.

3.3.2 The non-unital cases with either $w_1 = 0$ or $w_2 = 0$

We start by considering $\mathbf{w} = (0, w_2)$, $|w_2| \leq 1$, $w_2 \neq 0$. This means that the shift occurs only in the direction of the λ_2 -axis. In this case the χ -matrix is

$$\chi_{C_D}(\lambda_1, \lambda_2, w_2) = \frac{1}{2} \begin{pmatrix} 1 + \lambda_1 + \lambda_2 & 0 & w_2 \\ 0 & 1 + \lambda_1 - \lambda_2 & 0 \\ w_2 & 0 & 1 - \lambda_1 + \lambda_2 \end{pmatrix}.$$

First of all we notice that the condition $q_j \geq 0$ for $j = 0, 1, 2$ is still a necessary condition for positive semi-definiteness of the matrix and hence for complete positivity of C_D . This can be seen by selecting the vectors e_j of the canonical basis of \mathbb{R}^3 and performing the scalar product $e_j^\dagger \chi_{C_D}(\lambda_1, \lambda_2, w_2) e_j$, which reproduces exactly the values q_j , $j = 1, 2, 3$.

In order to give also sufficient conditions we compute the eigenvalues of this matrix. The characteristic polynomial of χ_{C_D} is:

$$P(x) = \left[\frac{1}{2}(1 + \lambda_1 - \lambda_2) - x \right] \left[x - \frac{1}{2} \left(1 + \lambda_2 + \sqrt{\lambda_1^2 + w_2^2} \right) \right] \left[x - \frac{1}{2} \left(1 + \lambda_2 - \sqrt{\lambda_1^2 + w_2^2} \right) \right], \quad (42)$$

and therefore the three eigenvalues are

$$\begin{cases} \mu_0 := \frac{1}{2}(1 + \lambda_1 - \lambda_2) \\ \mu_{\pm} := \frac{1}{2} \left(1 + \lambda_2 \pm \sqrt{\lambda_1^2 + w_2^2} \right). \end{cases}$$

The condition $\mu_0 \geq 0$ is equivalent to the necessary condition $q_1 \geq 0$ and the request that $\mu_{+} \geq 0$ gives $\lambda_2 \geq -\sqrt{\lambda_1^2 + w_2^2} - 1$, which is always true, since it is necessary that $|\lambda_j| \leq 1$ and $|w_j| \leq 1$ for all $j = 1, 2$ in order to guarantee positivity.

Finally, $\mu_{-} \geq 0$ gives $1 + \lambda_2 \geq \sqrt{\lambda_1^2 + w_2^2}$, which, squaring both sides gives an upper bound on w_2 , i.e. on the possible vertical shifts of the ellipsoid, precisely:

$$w_2^2 \leq (\lambda_2 + 1)^2 - \lambda_1^2. \quad (43)$$

The case in which $\mathbf{w} = (w_1, 0)$, i.e. when the shift occurs only in the λ_1 -axis, is analogous to the case described above. Proceeding as before, we obtain the following upper bound on the possible horizontal shifts of the ellipsoid:

$$w_1^2 \leq (\lambda_1 + 1)^2 - \lambda_2^2. \quad (44)$$

3.3.3 The non-unital case with a generic $\mathbf{w} = (w_1, w_2)$

In the general case, even if it is possible to compute the eigenvalues of χ_{C_D} , their explicit expression is so complicated that their non-negativity cannot be studied analytically. We can avoid this problem by studying the characteristic polynomial of the expression of χ_{C_D} in eq. (39), i.e.

$$P(x) = -x^3 + \frac{a}{2}x^2 - \frac{b}{4}x + \det(\chi_{C_D}), \quad (45)$$

with $a = 3 + \lambda_1 + \lambda_2$, $b = 3 - (w_1^2 + w_2^2) + 2(\lambda_1 + \lambda_2) - (\lambda_1 + \lambda_2)^2$ and

$$\det(\chi_{C_D}) = \frac{1}{8} \left[(1 - \lambda_1 + \lambda_2) \left[(1 + \lambda_1 + \lambda_2)(1 + \lambda_1 - \lambda_2) - w_1^2 \right] - w_2^2(1 + \lambda_1 - \lambda_2) \right]. \quad (46)$$

By Descartes' rule of signs, all the three roots of P are positive if and only if the coefficients of the powers of x present three variations, i.e. their signs change from one to the next. This happens if and only if a, b and $\det(\chi_{C_D})$ are all ≥ 0 .

Since the condition $|\lambda_j| \leq 1$ must hold to guarantee positivity, $a \geq 0$ always holds. The request $b \geq 0$ gives an upper bound on the norm of \mathbf{w} , that is

$$\|\mathbf{w}\|^2 = w_1^2 + w_2^2 \leq 3 + 2(\lambda_1 + \lambda_2) - (\lambda_1 + \lambda_2)^2. \quad (47)$$

Finally, $\det(\chi_{C_D}) \geq 0$ holds if and only if

$$w_1^2(1 - \lambda_1 + \lambda_2) + w_2^2(1 + \lambda_1 - \lambda_2) \leq (1 + \lambda_1 + \lambda_2)(1 + \lambda_1 - \lambda_2)(1 - \lambda_1 + \lambda_2) = 8q_0q_1q_2, \quad (48)$$

having used definition (40) in the last equality. The condition $\det(\chi_{C_D}) \geq 0$ always implies $b \geq 0$. Indeed, the region described by (47) is a disk w.r.t. the two variables (w_1, w_2) , moreover

$$\max_{|\lambda_j| \leq 1, j=1,2} \{3 + 2(\lambda_1 + \lambda_2) - (\lambda_1 + \lambda_2)^2\} = 4, \quad (49)$$

so the ray of this disk is always ≤ 2 . On the other hand, when $1 \pm \lambda_1 + \lambda_2 > 0$ and $1 + \lambda_1 - \lambda_2 > 0$, the region described by (48) w.r.t (w_1, w_2) is an ellipsoid that can be explicitly written as

$$\frac{w_1^2}{\frac{1}{4}(1 + \lambda_1 + \lambda_2)(1 + \lambda_1 - \lambda_2)} + \frac{w_2^2}{\frac{1}{4}(1 + \lambda_1 + \lambda_2)(1 - \lambda_1 + \lambda_2)} \leq 4. \quad (50)$$

Therefore, since

$$\max_{|\lambda_j| \leq 1, j=1,2} \{(1 + \lambda_1 + \lambda_2)(1 + \lambda_1 - \lambda_2)\} = \max_{|\lambda_j| \leq 1, j=1,2} \{(1 + \lambda_1 + \lambda_2)(1 - \lambda_1 + \lambda_2)\} = 4, \quad (51)$$

it follows that both denominators of the inequality (50) are bounded by 1 when $|\lambda_j| \leq 1$, $j = 1, 2$. This means that this ellipsoid described by the condition (50) is always contained into the disk described by eq. (47). Moreover, inequality (50) gives a nice geometric characterization of condition (48), saying that C_D is completely positive if and only if its shift vector \mathbf{w} belongs to the ellipsoid described by (50).

Notice that when $(1 - \lambda_1 + \lambda_2) = 0$ (or $(1 + \lambda_1 - \lambda_2) = 0$, or $(1 + \lambda_1 + \lambda_2) = 0$, respectively), inequality (48) forces $w_2 = 0$ (or $w_1 = 0$, or $w_1 = w_2 = 0$, respectively) and hence the ellipsoid described by inequality (48) degenerates to a segment or to the origin $(w_1, w_2) = \mathbf{0}$ which are always contained into the disk described by eq. (47).

In conclusion, $\det(\chi_{C_D}) \geq 0$ implies $b \geq 0$ in every case, and hence the inequality (48) is necessary and sufficient to guarantee that the eigenvalues of χ_{C_D} are ≥ 0 .

3.4 The classification theorem of rebit channels

We summarize the analysis conducted above in the following theorem.

Theorem 3.2 *Every rebit channel C can be decomposed as $C = \sigma_{\Omega_{\mathcal{R}_1}} \circ C_D \circ \sigma_{\Omega_{\mathcal{R}_2}}$, where $\sigma_{\Omega_{\mathcal{R}_j}}$ are orthogonal channels associated to the rotation matrices $\mathcal{R}_j \in \text{SO}(2)$, $j = 1, 2$, and C_D can be represented in the Bloch basis $(\sigma_0, \sigma_1, \sigma_2)$ by the affine matrix*

$$\mathbb{A} = \begin{pmatrix} 1 & 0 & 0 \\ w_1 & \lambda_1 & 0 \\ w_2 & 0 & \lambda_2 \end{pmatrix} = \begin{pmatrix} 1 & \mathbf{0} \\ \mathbf{w} & D \end{pmatrix},$$

with the coefficients λ_j, w_j , $j = 1, 2$, satisfying the following conditions:

$$\begin{cases} q_1 = 1 + \lambda_1 + \lambda_2 \geq 0 \\ q_2 = 1 + \lambda_1 - \lambda_2 \geq 0 \\ q_3 = 1 - \lambda_1 + \lambda_2 \geq 0 \\ \frac{w_1^2}{(1 + \lambda_1 + \lambda_2)(1 + \lambda_1 - \lambda_2)} + \frac{w_2^2}{(1 + \lambda_1 + \lambda_2)(1 - \lambda_1 + \lambda_2)} \leq 1 \end{cases} \quad (52)$$

Geometrically, because of the presence of C_D , the action of C on the Bloch disk representing the state space of the rebit is to shrink it to an ellipsoidal region contained in the unit disk in \mathbb{R}^2 , which can also degenerate into a line segment or in a point. Either the semi-axes of the ellipsoidal region or the line segment can be tilted with respect to the coordinate axes due to the presence of the orthogonal channels $\sigma_{\Omega_{\mathcal{R}_j}}$, $j = 1, 2$.

4 A basic recap of the quantum-like colour perception model

As declared in the introduction, we want to strengthen the importance of the theoretical result that we have just obtained by showing how it can be directly applied to the colour perception model developed in the papers [4, 2, 7, 5, 3, 8, 6]. The content of these papers is of course too

large to be reported entirely, for this reason here we will outline only the most important concepts and results that will be needed to understand why rebit channels appear in this theory.

In the second part of the nineteenth century it became clear, in particular to Riemann, Maxwell, Grassmann and von Helmholtz, that the space of perceptual colours \mathcal{C} is not merely a set of sensations, but a space with a rich mathematical structure. In [17], Schrödinger condensed the fragmented colour knowledge into a set of axioms which imply that \mathcal{C} is a 3-dimensional regular convex cone. \mathcal{C} represents an *ideal space of perceptual colours in isolation*, i.e. all the possible colour sensations reported by an observer exposed to a single light source in isolation without considering the so-called skotopic threshold and the glare limits, which are the lower and upper bounds of human sight with respect to the intensity of light stimuli.

In [15], Resnikoff completed Schrödinger's axiomatic system by exhibiting the homogeneity of \mathcal{C} and then proved that \mathcal{C} can only be either $[0, +\infty)^3$ or $[0, +\infty) \times \mathbf{H}$, where \mathbf{H} is a 2-dimensional hyperbolic space, see [14] for more details. The space $[0, +\infty)^3$ is the prototype of the classical CIE (Commission Internationale de l'Éclairage) colour spaces, whereas $[0, +\infty) \times \mathbf{H}$ is a much more interesting space from an algebraic, geometric and also perceptual point of view. $[0, +\infty) \times \mathbf{H}$ is isomorphic to $\overline{\mathcal{H}^+}(2, \mathbb{R})$, the space of 2×2 positive-semidefinite real symmetric matrices, and to $\overline{\mathcal{L}^+}$, the closed future lightcone in the 3-dimensional Minkowski space.

From now on, we will identify \mathcal{C} with either $\overline{\mathcal{H}^+}(2, \mathbb{R})$ or $\overline{\mathcal{L}^+}$, which coincide precisely with *the domain of positivity of the only two non-associative 3-dimensional formally real Jordan algebras*: $\mathcal{H}(2, \mathbb{R})$, composed by real symmetric 2×2 matrices, and $\mathbb{R} \oplus \mathbb{R}^2$, the so-called spin factor, both endowed with suitable Jordan products. For more information about Jordan algebras, the very clear paper [1] can be consulted, for the purposes of this paper the only result that we need to recall is that $\mathcal{H}(2, \mathbb{R})$ and $\mathbb{R} \oplus \mathbb{R}^2$ are isomorphic as Jordan algebras via the following natural map:

$$J: \quad \mathcal{H}(2, \mathbb{R}) \quad \xrightarrow{\sim} \quad \mathbb{R} \oplus \mathbb{R}^2$$

$$A = \begin{pmatrix} \alpha + v_1 & v_2 \\ v_2 & \alpha - v_1 \end{pmatrix} \quad \mapsto \quad J(A) = \begin{pmatrix} \alpha \\ v_1 \\ v_2 \end{pmatrix} \equiv \begin{pmatrix} \alpha \\ \mathbf{v} \end{pmatrix}. \quad (53)$$

Our assumption about \mathcal{C} is called *trichromacy axiom* because it is the mathematical translation of the trichromatic nature of human colour perception due to the existence of three retinal photoreceptors with different sensitivities. However, as it is well-known (see e.g. [9]), while photoreceptors *allow* colour vision, ganglion cells and other retinal neurons *generate* colour vision via the opponent mechanism first argued by Hering [12]. Thus, the properties of a perceptual colour space should be able to account for *both trichromacy and opponency*.

As we are going to see, this task can be intrinsically accomplished if we analyze colour perception with the mathematical formalism of quantum theories. The first step of the quantum-like colour perception theory consists in considering \mathcal{C} as the state cone of the model, i.e. as the set of states modulo a non-negative real constant. We represent quantum states \mathbf{s} via density matrices, which, in this framework, are unit trace matrices belonging to $\overline{\mathcal{H}^+}(2, \mathbb{R})$, explicitly,

$$\mathcal{S} = \left\{ \rho_{\mathbf{s}}(s_1, s_2) \equiv \frac{1}{2} \begin{pmatrix} 1 + s_1 & s_2 \\ s_2 & 1 - s_1 \end{pmatrix}, s_1^2 + s_2^2 \leq 1 \right\} \cong \mathcal{D}, \quad (54)$$

where \mathcal{D} is the unit disk in \mathbb{R}^2 , i.e. the state space of the rebit, which *emerges spontaneously* from the trichromacy axiom. Far from being an accidental (or even unwanted) feature of this model, the fact that chromatic states are labelled by elements of a 2-dimensional space is perfectly coherent with Hering's theory: the only intrinsic information that can be extracted by the observation of colours in isolation is represented by the two degrees of chromatic opposition, while the perceived intensity, or brightness, needs comparisons with other stimuli, see e.g. [13]. For this reason, we call *Hering's rebit* the system whose states are described by \mathcal{S} . The two degrees of opposition are exhibited by the density matrices when they are written in the Bloch representation, i.e.

$$\rho_{\mathbf{s}}(s_1, s_2) = \rho_0 + \frac{s_1}{2} \sigma_1 + \frac{s_2}{2} \sigma_2 \equiv \rho_0 + \frac{1}{2} \mathbf{v}_{\mathbf{s}} \cdot \vec{\sigma}, \quad (55)$$

where $\rho_0 := I_2/2$ and $\mathbf{v}_s \in \mathcal{D}$ indicates the Bloch vector. Using polar coordinates, i.e. $r \in [0, 1]$, $\vartheta \in [0, 2\pi)$ and $(s_1, s_2) = (r \cos \vartheta, r \sin \vartheta)$, one easily finds that

$$\rho_s(r, \vartheta) = \rho_0 + \frac{r \cos \vartheta}{2} [\rho(1, 0) - \rho(1, \pi)] + \frac{r \sin \vartheta}{2} \left[\rho\left(1, \frac{\pi}{2}\right) - \rho\left(1, \frac{3\pi}{2}\right) \right]. \quad (56)$$

It turns out that, for all ϑ , $\rho(1, \vartheta)$ is a rank-1 projector, i.e. a *pure state*, and $\rho(1, \vartheta_1)$, $\rho(1, \vartheta_2)$ project on orthogonal directions precisely when ϑ_1 and ϑ_2 are antipodal. Since orthogonality in quantum theories represents incompatible states, eq. (56) codifies a generic chromatic state as the superposition of two opponencies between incompatible states, red-green and yellow-blue in Hering's theory, plus an offset state represented by ρ_0 , called *achromatic state*, characterized by the fact of maximizing the von Neumann entropy and not carrying any chromatic information. For more information about the von Neumann entropy and its use in this colour perception model see in particular [6].

The picture in Figure 2 summarizes what recalled so far and translates in a rigorous setting the famous Newton colours disk.

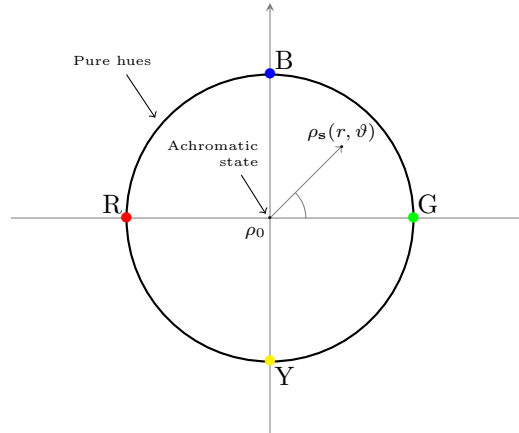


Figure 2: The space of chromatic states of Hering's rebit and its features.

Once obtained the chromatic state space \mathcal{S} , the state cone \mathcal{C}_s , isomorphic to $\overline{\mathcal{H}^+}(2, \mathbb{R})$, is

$$\mathcal{C}_s := \left\{ 2\alpha\rho_s = \begin{pmatrix} \alpha(1 + s_1) & \alpha s_2 \\ \alpha s_2 & \alpha(1 - s_1) \end{pmatrix}, \alpha \geq 0, \mathbf{v}_s = (s_1, s_2) \in \mathcal{D} \right\}. \quad (57)$$

Naively, one may guess that the direct interpretation of $\alpha \geq 0$ is the brightness of a perceptual colour, i.e. its perceived luminance. However, despite the fact that $[0, +\infty)$ surely contains the brightness values, the upper and lower perceptual bounds of human sight impose a restriction on the brightness values which turns the infinite state cone \mathcal{C}_s into a compact space called *colour solid*. Several proposals of colour solid can be found in the literature, the most famous being Mayer's and Lambert's double and single pyramid, respectively, Runge's sphere and Ostwald's double cone. None of them is based on a mathematical theory, but just on the proponent's intuition.

One of the great achievements of the quantum-like theory of colour perception is a rigorous solution to the long-lasting problem of reducing the infinite perceptual colour cone \mathcal{C} to a compact space and also defining brightness consistently with the structure of the resulting colour solid.

This solution makes use of the fundamental concepts of quantum effect and channel, which have been adapted with great formal rigor to colour perception in [8].

The notion of *effect* is related to the probabilistic interpretation of observable measurement when a system has been prepared in a given state. In the quantum-like colour perception model, an effect is a triple

$$\mathbf{e} := (e_0, \mathbf{v}_e), \quad (58)$$

where $e_0 \in \mathbb{R}$ is called effect magnitude and

$$\mathbf{v}_e := \begin{pmatrix} e_1 & e_2 \\ e_0 & e_0 \end{pmatrix}, \quad (59)$$

$e_1, e_2 \in \mathbb{R}$, is called *effect vector*, subjected to the condition that the *effect matrix*

$$\eta_e = \begin{pmatrix} e_0 + e_1 & e_2 \\ e_2 & e_0 - e_1 \end{pmatrix} \in \overline{\mathcal{H}^+}(2, \mathbb{R}), \quad (60)$$

is bounded between the null matrix and I_2 . This implies that $e_0 \in [0, 1]$ and

$$e_1^2 + e_2^2 \leq \min_{e_0 \in [0, 1]} \{(1 - e_0)^2, e_0^2\} \quad (61)$$

so, in particular, $\mathbf{v}_e \in \mathcal{D}$ and the space of all effects \mathcal{E} is the closed convex double cone with a circular basis of radius $1/2$ located height $\alpha = 1/2$, with vertices in $(e_0, e_1, e_2) = (0, 0, 0)$ and $(e_0, e_1, e_2) = (1, 0, 0)$, depicted in Figure 3 and in perfect agreement with the geometry of Ostwald's colour solid.

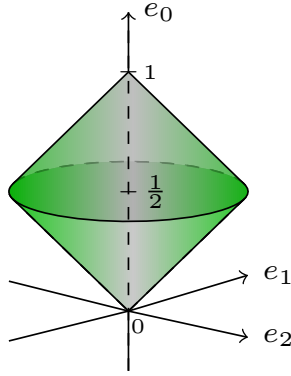


Figure 3: The convex double cone representing the effect space.

Following the quantum paradigm, it is natural to identify *the act of perceiving a colour*, interpreted as a *perceptual measurement*, with an effect. As a direct consequence, the colour solid of actually perceivable colours is identified with \mathcal{E} .

Crucially, after a measurement associated to an effect, the state of a system changes. Such state transformations are codified by the so-called *Lüders operations*, defined as follows: if the original state \mathbf{s} of a visual scene is described by the density matrix $\rho_{\mathbf{s}}$, then the measurement of a perceived colour, identified with the effect \mathbf{e} and represented by the matrix η_e , provokes a change of the initial state \mathbf{s} which becomes a *post-measurement generalized state* given by

$$\psi_e(\mathbf{s}) := \eta_e^{1/2} \rho_{\mathbf{s}} \eta_e^{1/2}, \quad (62)$$

$\eta_e^{1/2}$ is called the *Kraus operator* associated to the Lüders operation ψ_e and it is the square root of η_e , i.e. the only positive semi-definite matrix such that $\eta_e^{1/2} \eta_e^{1/2} = \eta_e$. Thanks to the cyclic property of the trace we have:

$$\text{Tr}(\psi_e(\mathbf{s})) = \text{Tr}(\rho_{\mathbf{s}} \eta_e) = \langle \mathbf{e} \rangle_{\mathbf{s}} = e_0(1 + \mathbf{v}_e \cdot \mathbf{v}_{\mathbf{s}}), \quad (63)$$

where $\langle \mathbf{e} \rangle_{\mathbf{s}}$ is the expectation value of the effect \mathbf{e} on the state \mathbf{s} . This implies that

$$\varphi_e(\mathbf{s}) = \frac{\psi_e(\mathbf{s})}{\langle \mathbf{e} \rangle_{\mathbf{s}}}, \quad (64)$$

is a density matrix representing the post-measurement state and the transformation $\rho_{\mathbf{s}} \mapsto \varphi_{\mathbf{e}}(\mathbf{s})$ is a rebit channel, called *Lüders channel*.

In [8] it has been proven that

$$J(\varphi_{\mathbf{e}}(\mathbf{s})) = \frac{1}{2} \begin{pmatrix} 1 \\ \mathbf{v}_{\mathbf{e}} \oplus \mathbf{v}_{\mathbf{s}} \end{pmatrix}, \quad (65)$$

where J is the isomorphism defined in (53) and \oplus denotes the Einstein-Poincaré relativistic sum between the two vectors, i.e. $\mathbf{v}_{\mathbf{e}} \oplus \mathbf{v}_{\mathbf{s}} = \mathbf{v}_{\mathbf{e}}$ if $\|\mathbf{v}_{\mathbf{e}}\| = 1$, otherwise

$$\mathbf{v}_{\mathbf{e}} \oplus \mathbf{v}_{\mathbf{s}} = \frac{1}{1 + \mathbf{v}_{\mathbf{e}} \cdot \mathbf{v}_{\mathbf{s}}} \left\{ \mathbf{v}_{\mathbf{e}} + \frac{1}{\gamma_{\mathbf{v}_{\mathbf{e}}}} \mathbf{v}_{\mathbf{s}} + \frac{\gamma_{\mathbf{v}_{\mathbf{e}}}}{1 + \gamma_{\mathbf{v}_{\mathbf{e}}} (\mathbf{v}_{\mathbf{e}} \cdot \mathbf{v}_{\mathbf{s}})} \mathbf{v}_{\mathbf{e}} \right\}, \quad (66)$$

where ‘ \cdot ’ denotes the Euclidean inner product and $\gamma_{\mathbf{v}_{\mathbf{e}}}$ is the \mathbf{e} -Lorentz factor, i.e.

$$\gamma_{\mathbf{v}_{\mathbf{e}}} = \frac{1}{\sqrt{1 - \|\mathbf{v}_{\mathbf{e}}\|^2}}. \quad (67)$$

The generalized density matrix $\psi_{\mathbf{e}}(\mathbf{s})$ contains both the chromatic information expressed by the state $\varphi_{\mathbf{e}}(\mathbf{s})$ and the normalized scalar information given by $\langle \mathbf{e} \rangle_{\mathbf{s}}$. In [6] a perceived colour associated to a measurement labelled by an effect \mathbf{e} has been defined precisely as the post-measurement generalized state $\psi_{\mathbf{e}}(\mathbf{s})$ and its brightness as $\text{Tr}(\psi_{\mathbf{e}}(\mathbf{s})) = \langle \mathbf{e} \rangle_{\mathbf{s}}$. This definition not only fits ideally with the quantum paradigm, but it has also been proven to provide a rigorous description of the lightness constancy property of human vision, see again [6] for more details.

To recap, the infinite cone \mathcal{C} , which can be identified with the state cone of an ideal observer without perceptual bounds, reduces to the compact double cone \mathcal{E} when the limitations of real human sight are taken into account.

5 Applications of the rebit channels classification to colour perception

Even if the description of perceived colours as elements of \mathcal{E} is much more realistic than the one offered by the infinite state cone $\mathcal{C}_{\mathbf{s}}$, there is still a degree of idealisation left: the chromatic state space \mathcal{S} , parametrized by the elements of the Bloch disk, refers to an observer without any degree of colour deficiency. As it is well-known, retinal photoreceptors may have spectral sensitivity distributions that deviate from the standard ones due to genetic or acquired anomalies, or they may even be absent. These pathological conditions lead to colour deficiencies such as anomalous trichromacy, dichromacy or total colour blindness, see e.g. [10, 18] for more information. In these cases, not all the chromatic states are attainable. In fact, evidences about variations in the subjective ability to discern and categorise colours indicate that *each observer*, after measuring a colour, *leaves a perceptual signature on the chromatic state space* by modifying it accordingly to the particular features of her/his visual system.

This consideration is the key to understand the usefulness of Hering’s rebit channels classification: since the act of perceiving a colour is modelled by the Lüders channel associated to the effect \mathbf{o} representing a given observer, *the possible chromatic states perceived by the observer \mathbf{o} must be searched in the deformed state spaces of the Bloch disk after the application of the Lüders channel $\varphi_{\mathbf{o}}$* . We formalise this sentence as follows.

Def. 5.1 *The individual chromatic state space $\mathcal{I}_{\mathbf{o}}$ of an observer modelled by the effect \mathbf{o} is the range of the Lüders channel $\varphi_{\mathbf{o}}$, i.e.*

$$\mathcal{I}_{\mathbf{o}} = \{\varphi_{\mathbf{o}}(\mathbf{s}), \mathbf{s} \in \mathcal{S}\}, \quad (68)$$

where \mathcal{S} has been defined in (54).

Experimentally, \mathcal{I}_\circ can be obtained through the so-called hue scaling experiments, in which an observer is asked to judge the proportion of opposition red-green and yellow-blue that he or she perceives in a given light stimulus presented in isolated conditions (i.e. without other light stimuli and no external illumination), see [10] for more details. Experimental evidence tells us that, in such conditions, the Lüders channel φ_\circ is unital, i.e. the achromatic state is preserved. For this reasons, in the following subsection, we will study the possible individual chromatic state spaces by analysing only the most relevant cases of unital rebit channels.

5.1 Categorisation of human observers

In section 3 we have seen that the really interesting information about the deformation of the Bloch disk by a unital rebit channel is contained in way the scaling parameters λ_1, λ_2 vary inside the admissible region \mathcal{P} depicted in Figure 1 and described by inequalities (41). In fact, the presence of the orthogonal channels appearing in theorem 3.2 simply amounts to a rotation of the Bloch vectors. So, in what follows, we will just concentrate on diagonal unital channels C_D , recalling that their action on a general state $\rho_s = \frac{1}{2}(\sigma_0 + r \cos(\vartheta)\sigma_1 + r \sin(\vartheta)\sigma_2)$ is the following:

$$\begin{pmatrix} 1 & 0 & 0 \\ 0 & \lambda_1 & 0 \\ 0 & 0 & \lambda_2 \end{pmatrix} \frac{1}{2} \begin{pmatrix} 1 \\ r \cos(\vartheta) \\ r \sin(\vartheta) \end{pmatrix} = \frac{1}{2} \begin{pmatrix} 1 \\ \lambda_1 r \cos(\vartheta) \\ \lambda_2 r \sin(\vartheta) \end{pmatrix}. \quad (69)$$

Let us start by the characterisation of the so-called *Kraus rank* of C_D , i.e. the number of non-zero eigenvalues of the associated χ -matrix:

- the vertices of \mathcal{P} given by $(\lambda_1, \lambda_2) = (-1, 0)$ and $(\lambda_1, \lambda_2) = (0, -1)$ correspond to *rank-1* channels because $q_1 = q_2 = 0, q_3 = 2$ and $q_1 = q_3 = 0, q_2 = 2$, respectively;
- the points belonging to the three diagonal edges of \mathcal{P} defined by the conditions $\lambda_2 = \pm\lambda_1 - 1$ and $\lambda_2 = \lambda_1 + 1$ correspond to *rank-2* channels. This is straightforward to see, since a single vanishing eigenvalue q_j in eq. (40) defines a diagonal edge, and so the intersection of two diagonal edges correspond to two vanishing eigenvalues;
- all the other points of \mathcal{P} correspond to *full-rank* (i.e. rank-3) channels.

Now we pass to the analysis of some noticeable Hering's rebit channel.

1. The *identity channel*, which correspond to $(\lambda_1, \lambda_2) = (1, 1)$, leaves the Bloch disk invariant. This is the only channel with this behaviour. In fact, apart from the case just examined, the length of the disk axes could be preserved only by the couples $(-1, -1), (1, -1), (-1, 1)$ which, however, lie outside the admissibility region \mathcal{P} .
2. The *phase flip channels*: by substituting $(\lambda_1, \lambda_2) = (1 - p, 1)$, with $0 < p < 1$, in eq. (69), the corresponding channels transform the Bloch disk into an ellipsoid that intersects it at the poles, i.e. yellow and blue of Figure 2, which remain fixed, while the disk is shrunk in the red-green direction. The case $p = 1$, i.e. $(\lambda_1, \lambda_2) = (0, 1)$, corresponds to a rank-2 channel which reduces the Bloch disk to the yellow-blue opponent axis.

The case $(\lambda_1, \lambda_2) = (1, 1 - p)$ is exactly analogous, with the role of the two opponent axes swapped, hence such channels have the red and green points of the Bloch disk fixed and shrink the disk in the yellow-blue direction. When $p = 1$ the Bloch disk degenerates into the green-red opponent axis. Figure 4 illustrates all these cases.

3. *Depolarizing channels* are channel such that $|\lambda_1| = |\lambda_2|$, i.e. corresponding to points lying on the two bisectors of \mathcal{P} in Figure 1. These channels simply shrink the Bloch disk to another disk with radius $r < 1$. If one of the λ_j 's is negative, the channel reflects also the disk with respect to one of the two (or both) axes. When $\lambda_1 = \lambda_2 = 0$, the entire disk degenerates to the single central point, i.e. the achromatic state. This is the so-called *completely depolarizing channel*.

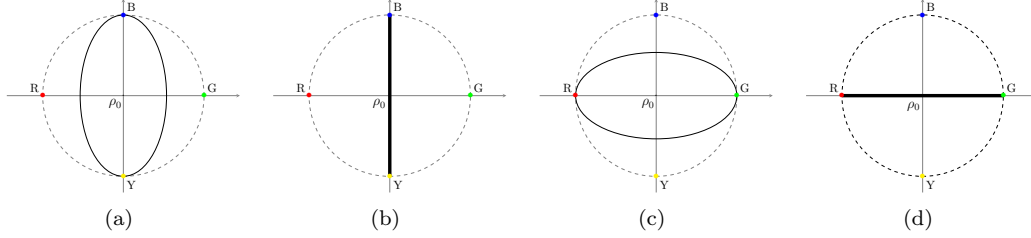


Figure 4: (λ_1, λ_2) for phase flip channels. (a): $(1 - p, 1)$, (b): $(0, 1)$, (c): $(1, 1 - p)$, (d): $(1, 0)$, $p \in (0, 1)$.

4. *Linear channels* are defined by the condition that either λ_1 or λ_2 or both are equal to 0, i.e. they correspond to points lying on the horizontal or vertical axis in Figure 1. When $(\lambda_1, \lambda_2) = (q, 0)$ (or $(\lambda_1, \lambda_2) = (0, q)$, respectively), with $-1 < q < 1$, the entire Bloch disk is sent to an horizontal (or vertical, respectively) segment of length $2|q|$. When $q < 0$ also a reflection is applied. When $q = 0$ we recover the completely depolarizing channel.

When $q = -1$ we have the two rank-1 channels corresponding to the vertices $(0, -1)$ and $(-1, 0)$, which are the intersection of two of the diagonal edges. These channels first shrink the Bloch disk to a segment as in case 2., but in addition they reflect it with respect to the horizontal or vertical axis, respectively.

5. All the other channels correspond to points lying either on the ‘diagonal’ edges or to the interior of Figure 1. In the first case we have rank-2 channels, in the second one full-rank channels. All the corresponding channels transform the Bloch disk to a generic ellipsoid.

Figure 5 gives a compact illustration of the channels discussed in the previous list depending on the position of the couple of scaling parameters $(\lambda_1, \lambda_2) \in \mathcal{P}$. Due to theorem 3.1, the previously discussed transformations of the Bloch disk must be considered up to rotations.

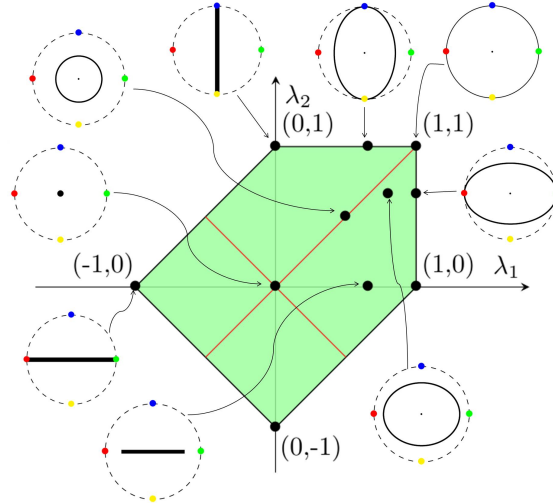


Figure 5: A visual representation of the cases described in the previous list. Starting from the identity and proceeding in a clockwise ordering we have: a phase flip of the type $(\lambda_1, \lambda_2) = (1, 1 - p)$, a general case, a linear channel, a rank-1 degenerate channel, the completely depolarizing channel, a depolarizing channel, a degenerate phase flip and finally a phase flip of the type $(\lambda_1, \lambda_2) = (1 - p, 1)$.

Thanks to eq. (66), we know that the relativistic sum $\mathbf{v}_o \oplus \mathbf{v}_s$, i.e. the Bloch vector relative to the post-measurement state produced by the perception of a chromatic state \mathbf{s} by an observer

modelled by the effect \mathbf{o} , will be contained in one of the deformed Bloch disks just discussed.

We are now able to give a mathematical characterisation of human observers by using the classification of unital Hering's rebit channels. To this aim, we recall some standard definitions from ophthalmology and colour theory:

- the LMS cones are the retinal photoreceptors with sensitivity pick in the long, middle and short wavelengths of the visual spectrum. Apart from the separation of their picks, the sensitivity curves of the L and M cones are almost identical and they vastly overlap;
- a *normal trichromatic observer* is a person with the three LMS cones functioning and with maxima of their absorption curves at 560, 530 and 420 nm, respectively;
- an *anomalous trichromatic observer* is a person with the three LMS cones functioning, but the absorption curves maxima of the L and M cones are less separated, between 2 and 12 nm, with respect to the 30 nm separation of normal trichromats. This is by far the most common colour deficiency found in humans. We further distinguish between the two following sub-categories: *protanomalous* have normal S and M cones, but anomalous L cones whose spectral sensitivity curve is shifted closer to that of M cones; *deuteranomalous* have normal S and L cones, but anomalous M cones whose spectral sensitivity curve is shifted closer to that of L cones³;
- a *dichromatic observer* is a person who lacks one type of cones. We distinguish among: *protanopes*, who lack the L cones; *deuteranopes*, who lack the M cones; *tritanopes*, who lack the S cones⁴;
- a *monochromatic observer* is a person affected by a very rare colour deficiency in which only the S cones are functioning or no cones at all, in which case they only possess skotopic vision via the rod system. These people totally lack chromatic sensation.

Let $(\lambda_1, \lambda_2) \in \mathcal{P}$ be the scale parameters corresponding to the Lüders channel $\rho_{\mathbf{s}} \mapsto \varphi_{\mathbf{o}}(\mathbf{s})$, where \mathbf{s} is a chromatic state. Then \mathbf{o} models:

- a *normal trichromatic observer* if $(\lambda_1, \lambda_2) = (1, 1)$, because in this case the Bloch disk remains preserved as a whole, so all the chromatic states can be perceived;
- an *anomalous trichromatic observer* if $(\lambda_1, \lambda_2) = (1 - p, q)$, $p \in (0, 1)$, $q \in (0, 1]$, $q > 1 - p$, i.e. if $\varphi_{\mathbf{o}}$ is a *phase flip* or a *depolarizing* channel that shrinks the Bloch disk more into the red-green direction. In this case, in fact, the neurons of the parvocellular pathway have more difficulty in performing the comparison between the output signals of the L and M cones, hence the red-green opposition axis gets shorter. The anomaly worsens as $p \rightarrow 1$;
- a *dichromatic observer* if (λ_1, λ_2) corresponds to a *linear channel* or a *degenerate rank-1 phase flip* channel, in particular:
 - if $(\lambda_1, \lambda_2) = (0, q)$, $q \in (0, 1]$, we have a *protanope* or a *deuteranope*;
 - if $(\lambda_1, \lambda_2) = (q, 0)$, $q \in (0, 1]$, we have a *tritanope*.

Both conditions become more severe as $q \rightarrow 0$;

- a *monochromatic observer* if $(\lambda_1, \lambda_2) = (0, 0)$ because in this case the only state that can be reported is the achromatic one, with variations in brightness.

³data on people with a shifted S cone spectral sensitivity have not been confirmed solidly.

⁴the prefixes used in these definitions and the following one are derived from *protos*, *deuteros* and *tritros*, which mean first, second and third, respectively, in ancient Greek.

5.2 Qualitative analysis of the adaptation to a non-neutral illuminant

Chromatic adaptation is the human visual system ability to modify colour perception when the spectral distribution of lighting varies in order to maintain as fixed as possible the perception of achromatic surfaces. This phenomenon can be experienced by everyone wearing, for instance, a ski mask: as soon as the mask is worn the snow seems yellowish, but after a short amount of time this sensation disappears and snow is perceived as achromatic. When the mask is removed, snow appears bluish for a few seconds under natural light conditions, before the achromatic sensation comes back.

Here we propose a qualitative discuss on the interpretation of chromatic adaptation in terms of Hering's rebit channels. In a future work, a quantitative analysis will complete the present one.

So far we have modelled mathematically the interaction between an observer and a visual scene prepared in a given chromatic state \mathbf{s} , represented by a light stimulus in isolated conditions, perceived by a human observer identified with an effect \mathbf{o} . When the visual scene consists in a patch lit by an illuminant, the mathematical description must be modified as thoroughly discussed in [6]: the physical properties of the patch define a chromatic state \mathbf{s} which is altered by the illuminant, modelled as a *physical effect* $\boldsymbol{\iota}$, which participates to the visual scene preparation.

We are now going to analyse two different situations that will provide possible explanations of the reason why the adaptation to illuminants slightly different than daylight is practically unnoticeable and, on the contrary, under extreme illuminant conditions, adaptation cannot restore a full chromatic vision.

Let us start with the first case by considering, for instance, an achromatic patch lit by a slightly yellowish illuminant. In this case $\mathbf{s} = \rho_0$, and, since the illuminant $\boldsymbol{\iota}$ is yellowish, the chromatic state presented to the observer will be $\varphi_{\boldsymbol{\iota}}(\rho_0)$, where $\varphi_{\boldsymbol{\iota}}$ is the non-unital Lüders channel associated to the action of the illuminant on the patch, which shifts ρ_0 vertically towards the south pole $(0, -1)$, where the pure yellow hue is locate, hence its shift vector is $\mathbf{w} = (0, w_2)$, $-1 < w_2 < 0$, $|w_2| \ll 1$. It is worth stressing again that what just described is still part of the scene preparation.

When the observer interacts with the visual scene prepared in this way, the sudden yellowish sensation provoked by $\varphi_{\boldsymbol{\iota}}(\rho_0)$ will rapidly be modified by her/his visual system to become the achromatic state of her/his own chromatic state space through the Lüders channel $\varphi_{\mathbf{o}}$. Figure 6 illustrates what just discussed and shows also that if the yellowish illuminant is replaced by a neutral one, the observer will suddenly perceive a bluish patch relative to the chromatic state $\tilde{\rho}$ with Bloch vector $\mathbf{v}^{\tilde{\rho}} = (0, -w_2)^t$, before rapidly experiencing again an achromatic sensation.

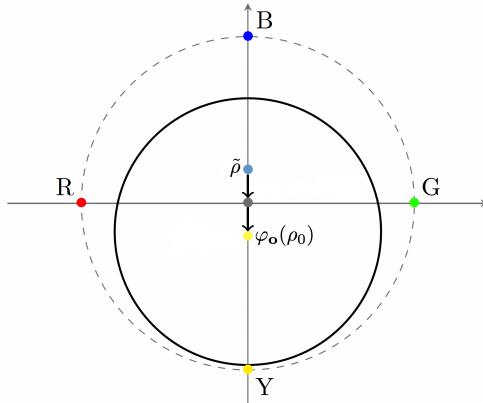


Figure 6: Illustration of the phenomenon of chromatic adaptation to a yellowish illuminant.

Now let us concentrate on the case in which the illuminant is not given by a slightly yellowish light, but a very saturated red one. In this case, when the observer adapts to this kind of situation, the channel $\varphi_{\mathbf{o}}$ shrinks dramatically the Bloch disk to a small ellipsoidal region close to the pure red border of the original Bloch disk, in order to remain inside it, as illustrated in Figure 7. In

this case, the amount of chromatic states that can be perceived will be very limited, as confirmed by the data reported in visual experiments performed with very saturated illuminants.

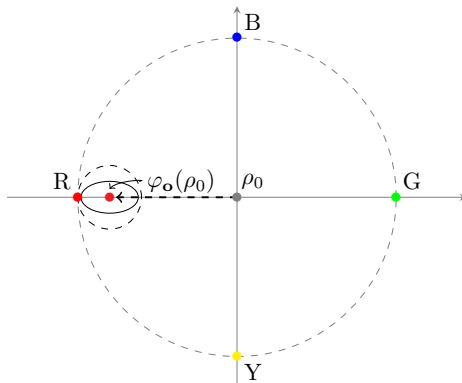


Figure 7: Illustration of the phenomenon of chromatic adaptation to a very saturated red illuminant.

6 Conclusions and perspectives

We have detailed the complete classification of rebit channels and underlined that the strategy used in the 2002 paper [16] for the classification of qubit channels, founded on Choi’s theorem, must be replaced by an alternative procedure based on the χ -matrix representation. This should not come as a surprise, because rebits properties cannot be deduced from those of qubits simply by replacing \mathbb{C} with \mathbb{R} : for instance, in [19] it is proven that local measurements are enough to determine the state of an open qubit system, but this is not always true for a rebit.

We have also shown that our classification result has not only a theoretical significance, but it has important applications in a recent quantum information-based model of colour perception. The surprising link between two apparently very distant research fields is offered by the fact that, in [8, 6], the act of perceiving colours by a human observer is described via rebit channels hence, by knowing how they modify the Bloch disk, it is possible to obtain an individual description of the chromatic state space for each observer. Remarkably, this technique permits to single out also colour deficiencies of different degree and type.

Finally, we have discussed how to apply the rebit channel classification to a qualitative interpretation of the phenomenon of visual adaptation to a non-neutral illuminant which is coherent with everyday experience. In a future work, we plan to deepen the study of this important perceptual feature with a quantitative analysis based on the concept of relative quantum entropy.

References

- [1] John C Baez. Division algebras and quantum theory. *Foundations of Physics*, 42(7):819–855, 2012.
- [2] M. Berthier. Geometry of color perception. Part 2: perceived colors from real quantum states and Hering’s rebit. *The Journal of Mathematical Neuroscience*, 10(1):1–25, 2020.
- [3] M. Berthier, V. Garcin, N. Prencipe, and E. Provenzi. The relativity of color perception. *Journal of Mathematical Psychology*, 103:102562, 2021.
- [4] M. Berthier and E. Provenzi. When geometry meets psycho-physics and quantum mechanics: Modern perspectives on the space of perceived colors. In *International Conference on Ge-*

ometric Science of Information 2019, volume 11712 of *Lecture Notes in Computer Science*, pages 621–630. Springer Berlin-Heidelberg, 2019.

- [5] M. Berthier and E. Provenzi. From Riemannian trichromacy to quantum color opponency via hyperbolicity. *Journal of Mathematical Imaging and Vision*, 63(6):681–688, 2021.
- [6] Michel Berthier, Nicoletta Prencipe, and Edoardo Provenzi. A quantum information-based refoundation of color perception concepts. *SIAM Journal on Imaging Sciences*, 15(4):1944–1976, 2022.
- [7] Michel Berthier and Edoardo Provenzi. The quantum nature of color perception: Uncertainty relations for chromatic opposition. *Journal of Imaging*, 7(40), 2021.
- [8] Michel Berthier and Edoardo Provenzi. Quantum measurement and colour perception: theory and applications. *Proceedings of the Royal Society A*, 478(2258):20210508, 2022.
- [9] R. L. de Valois and K. K. de Valois. Neural coding of color. In A. Byrne and D. R. Hilbert, editors, *Readings on Color, the Science of Color*, volume 2, pages 93–140. A Bradford Book, the MIT Press, Cambridge, Massachusetts, London, England, 1997.
- [10] Kara J Emery, Mohana Kuppaswamy Parthasarathy, Daniel S Joyce, and Michael A Webster. Color perception and compensation in color deficiencies assessed with hue scaling. *Vision Research*, 183:1–15, 2021.
- [11] Teiko Heinosaari and Mário Ziman. *The mathematical language of quantum theory: from uncertainty to entanglement*. Cambridge University Press, 2011.
- [12] Ewald Hering. *Zur Lehre vom Lichtsinne: sechs Mittheilungen an die Kaiserl. Akademie der Wissenschaften in Wien*. C. Gerold’s Sohn, 1878.
- [13] D.H. Hubel. *Eye, Brain, and Vision*. Scientific American Library, 1995.
- [14] Edoardo Provenzi. Geometry of color perception. Part 1: Structures and metrics of a homogeneous color space. *The Journal of Mathematical Neuroscience*, 10(1):1–19, 2020.
- [15] H.L. Resnikoff. Differential geometry and color perception. *Journal of Mathematical Biology*, 1:97–131, 1974.
- [16] Mary Beth Ruskai, Stanislaw Szarek, and Elisabeth Werner. An analysis of completely-positive trace-preserving maps on M_2 . *Linear algebra and its applications*, 347(1-3):159–187, 2002.
- [17] E. Schrödinger. Grundlinien einer theorie der farbenmetrik im tagessehen (Outline of a theory of colour measurement for daylight vision). Available in English in Sources of Colour Science, Ed. David L. Macadam, The MIT Press (1970), 134-82. *Annalen der Physik*, 63(4):397–456; 481–520, 1920.
- [18] T. Wachtler, T-W. Lee, and T.J. Sejnowski. Chromatic structure of natural scenes. *J. Opt. Soc. Am A*, 18(1):65–77, 2001.
- [19] William K Wootters. Local accessibility of quantum states. *Complexity, entropy and the physics of information*, 8:39–46, 1990.
- [20] William K Wootters. The rebit three-tangle and its relation to two-qubit entanglement. *Journal of Physics A: Mathematical and Theoretical*, 47(42):424037, 2014.